

This is the peer reviewed version of the following article:

Electron transfer in nanobiodevices / Alessandrini, Andrea; Facci, Paolo. - In: EUROPEAN POLYMER JOURNAL. - ISSN 0014-3057. - 83:(2016), pp. 450-466. [10.1016/j.eurpolymj.2016.03.028]

*Terms of use:*

The terms and conditions for the reuse of this version of the manuscript are specified in the publishing policy. For all terms of use and more information see the publisher's website.

07/05/2026 00:20

(Article begins on next page)

# Accepted Manuscript

Electron Transfer in Nanobiodevices

Andrea Alessandrini, Paolo Facci

PII: S0014-3057(16)30132-X

DOI: <http://dx.doi.org/10.1016/j.eurpolymj.2016.03.028>

Reference: EPJ 7295

To appear in: *European Polymer Journal*

Received Date: 19 October 2015

Revised Date: 11 March 2016

Accepted Date: 21 March 2016

Please cite this article as: Alessandrini, A., Facci, P., Electron Transfer in Nanobiodevices, *European Polymer Journal* (2016), doi: <http://dx.doi.org/10.1016/j.eurpolymj.2016.03.028>

This is a PDF file of an unedited manuscript that has been accepted for publication. As a service to our customers we are providing this early version of the manuscript. The manuscript will undergo copyediting, typesetting, and review of the resulting proof before it is published in its final form. Please note that during the production process errors may be discovered which could affect the content, and all legal disclaimers that apply to the journal pertain.



# Electron Transfer in Nanobiodevices

Andrea Alessandrini<sup>1,2</sup> & Paolo Facci<sup>3</sup>

<sup>1</sup>University of Modena and Reggio Emilia, Department of Physics, Informatics and Mathematics, Via Campi 213/A, 41125, Modena, Italy.

<sup>2</sup>CNR - Istituto Nanoscienze, S3, Via Campi 213/A, 41125, Italy.

<sup>3</sup>CNR - Istituto di Biofisica, Via De Marini 6, 16149, Genova, Italy.

## Abstract

The present tutorial is aimed at introducing the reader to the main aspects of electron transfer in nanobiodevices. Nanobiodevices are faced both from scientific and technological viewpoints and their particular implementation as electron transfer devices provides the opportunity of presenting fundamentals of electron transfer theory. Examples of implementations of stand alone devices, along with those involving reconfigurable set-ups based on an electrochemical scanning tunneling microscope, enable introducing heterogeneous electron transfer and electron transport theories in electrochemical environment. Specific cases of nanobiodevices involving redox metalloproteins are reported and experimental results are interpreted and discussed in view of the most recent theoretical advancements, in order to provide the reader with a comprehensive view of the results and promises in this exciting branch of nanotechnology.

## Introduction

Among the potential applications of nanotechnology, those arising from its merging with biological matter represent for sure some of the most appealing ones both from cultural and exploitation standpoints.

As for any other kind of matter, also that of biological origin matches the nanometer size at molecular level, that is, at the level of the dimensions characterizing the basic functional constituents of living beings. Nucleic acids and proteins, the most important biomolecular constituents, share this characteristic and have been often exploited in the realization of nanobiodevices [1].

Of course, devices that are intended for applications involving (single) functional biomolecules can be useful in, and impact on, several diverse fields ranging from healthcare [2] to food safety [3] to drug discovery [4], to biotechnology [5], to bioelectronics [6] and biosensing [7], just to quote some of the most relevant ones.

The interplay between nanotechnology and biological matter is, indeed, characterized by a sort of bidirectional link. On the one hand, the nanometer dimensional range is ideal for targeting and interacting with single biomolecules, whose size lies typically in that range; on the other hand, biological function is often inherent to single biomolecules that, as such, can deploy all their functional activity also in artificial, technological environments.

In the present tutorial, however, we will focus only on a special class of nanobiodevices, those involving molecules and mechanisms related to the phenomenon of electron transfer (ET) [8]. These nanobiodevices encompass both nanobioelectronic and nanobiosensor devices and rely mostly on a special class of biomolecules, that of redox metalloproteins [9].

These are proteins characterized by the presence of one or more redox centers involved in their functional activity. Usually, redox metalloprotein function is related to changes in oxidation state of the mentioned centers that play the role of electronic stations in phenomena where electron transfer determines the biological function. Examples of these phenomena range from enzymatic catalysis [10], to charge separation in early steps of photosynthesis [11], to electron shuttling among different redox partners during complex cascades of biochemical redox reactions accompanying respiration [12], and so on.

At any rate, electron transfer nanobiodevices are typically characterized by an electrode nanostructure, realized by top-down

(e.g. different kinds of lithographies, electrochemical etching) or bottom-up (e.g. self-assembly, electrochemically assisted deposition, molecular beam epitaxy) approaches, that interacts with single/few biomolecules properly located in the proximity of the electrode structure by self-assembly (e.g. specific interaction between partner pairs such as antibody-antigen, ligand-receptor), direct chemisorption (e.g Au-S bond formation) or dielectrophoresis.

The possible resulting structures can be self-contained, as in case of lithographed nanotransistors or electrochemical sensors, or assembled by reconfigurable tools such as the electrochemical scanning tunneling microscope (ECSTM), or conductive scanning force microscope (CSFM) [13].

Among the firsts, ultimate resolution lithographic techniques play a prominent role. Focused ion beam lithography (FIB) [14], electron beam lithography (EBL) [15], and molecular beam epitaxy (MBE) [16] techniques, coupled with specific etching procedures, are used to define either planar or vertical nanostructures usually characterized by nanometer gaps between electrodes, where single or few molecules can sit. Most often, a three-electrode structure is defined, where two electrodes play the role of drain and source electrodes, whereas a third control one plays the role of gate electrode in a fashion resembling a field effect transistor (FET). Lithographed electrode structures configure gaps that are not always tiny enough to accommodate a single molecule. That is why the lithographic approach is often complemented by electrochemically controlled metal deposition [17] or by other metal cluster localization techniques to reduce the gap size between drain and source electrodes down to molecular dimensions. Chemisorption, molecular recognition or dielectrophoresis [18] are then used to locate the molecule(s) of interest in the gap, possibly imparting also a desired orientation to it (them). Since we are dealing with biomolecules, it is often mandatory and always preferable to operate in a wet environment [6]. This fact poses further requirements to the electrode set-up that should enable measurements in salty water. Such a feature is usually not easily attainable in self-contained nanobiodevices, since it requires extensive insulation of all of the electrodes surface apart from the very tips of source and drain and the use of an external circuitry to drive independently the potentials of the two electrodes [8].

A ready solution to this problem is provided by a second class of architectures usable for assembling a nanobiodevice: that of scanning tunneling microscope with electrochemical control of the potential of the electrodes at play [19].

ECSTM is indeed a scanning tunneling microscope that can be operated in a salty liquid environment and that is assisted by an external bipotentiostat allowing to control the potential of the metal substrate and tip independently of each other (see below). This experimental set-up has been extensively used to characterize the flow of electrons via single redox metalloproteins [21] immobilized on a metal substrate as well as for configuring the physical equivalent of a single molecule transistor with an electrochemical gate [21]. Fundamental understanding of the physics of electron transport via surface immobilized redox metalloproteins, the role of the redox site oxidation state, as well as that of the particular metal ion in the active site have been elucidated by this technique along the last 15 years (see below). Theories accounting for the particular features observed when a redox metalloprotein is sandwiched between two nanoelectrodes and a flow of electrons through its redox center is gated electrochemically, have been developed (see below). Their interpretation of the experimental data has led to a robust understanding of the basic physical principles and, sometimes, complex mechanisms governing electron transport in surface immobilized redox metalloproteins, hence paving the way to the exploitation of these molecules and phenomena in functional nanobiodevices.

### **Fundamentals of electron transfer and heterogeneous electron transfer**

The process of electron transfer refers to the exchange of one electron between two partners, designated as the “donor” and the “acceptor”. In the following we will present a very brief description of the general electron transfer process, described from the point of view of the Marcus classical theory [22], and then we will concentrate on the aspects related to the electron transport phenomenon in single molecules which are relevant in the context of configurations based on Electrochemical Scanning Tunneling Microscopy. Excellent reviews on the topic of electron transfer in biosystems according to the Marcus theory are present in the literature and the reader are referred to these papers for a deeper understanding of the theory [23-26]. Before starting the description of the electron transfer process, it

is important to distinguish the electron transfer phenomenon from the electron transport one. Typically, the electron transfer process involves the presence of a donor, an acceptor and a molecular bridge connecting the two. The driving force for this process is related to partners' nuclear relaxation and to the reorganization of the solvent as described in the Marcus theory [22]. In contrast, the transport mechanism is usually based on the presence of two solid electrodes which are separated by a single, a few or a layer of molecules and the driving force for the electron flow is provided by a voltage difference between the two solid electrodes producing a flow of electrons by a non-equilibrium situation.

In the Marcus picture, a typical reaction which involves crossing an activation energy barrier is considered. The two minima represent the equilibrium configurations of reactants and products (they are different because the electron transfer process typically leads to a change in the configuration of nuclei) together with the solvent and their difference is the driving force for the reaction we are considering. Marcus assigned a parabolic shape to the energy diagrams describing the nuclei movement around the equilibrium position for both the reactants and the products (Figure 1). Before the electron transfer occurs, the electron occupies the HOMO of the donor and the energy of the donor and acceptor system is lower than the energy of the complex with the exchanged electron. At the intersection of the two curves the two energies are equal and the transfer can occur. If small distances are involved, the transfer mechanism is tunneling across the barrier separating the energy of the molecules before the transfer and the energy of the molecules after the transfer. The electron transfers from the HOMO of the donor to the LUMO of the acceptor. The rate of electron transfer is related to the overlap integral of the involved wave-functions. If the coupling is weak, the overlap Hamiltonian will undergo an exponential decrease as a function of distance with a characteristic length. The electron transfer rate will thus include a pre-factor that represents also the efficacy of the electron transfer through a specific material. A more complete treatment should include however quantum mechanical effects and nuclear tunneling together with electron tunneling, especially in the inverted region and in the case of strong coupling between reactants and products (see below). Considering the intersection point between the two parabolas, and assuming the two curves are just shifted in  $x$  and  $y$  directions, it emerges that its  $y$  value, associated with the activation energy for the reaction  $\Delta E$  and therefore with the reaction rate, is given by the following expression:

$$\Delta G^* = \frac{(\Delta G_0 + \lambda)^2}{4\lambda} \quad [1]$$

where  $\Delta G_0$  is the driving force for the reaction and  $\lambda$  is the reorganization energy, defined as the energy it would take to change the reactant coordinates to the same coordinates of the products but without letting the electron transfer occur. The reorganization energy is composed by an inner contribution related to the reorganization of reactant species and an outer sphere contribution due to the solvent reorganization. The electron transfer reaction must satisfy the Franck-Condon principle, which might be expressed as the condition in which electron transfer occurs without providing enough time for the corresponding nuclei movement. This condition can be considered as the requirement for a vertical transition in the free energy plot reported in Figure 1. Anyway, a vertical transition means that the

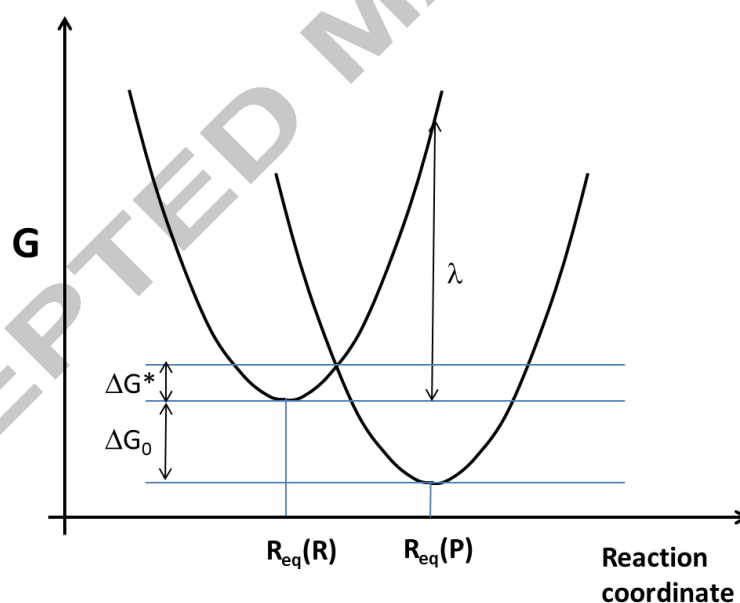


Figure 1: Energy diagram for the electron-transfer reaction between reactants (R) and products (P). The driving force for the reaction is the difference between the equilibrium energy of reactants and products ( $\Delta G_0$ ).  $\Delta G^*$  represents the activation energy for the reaction which determines the reaction rate.  $\lambda$  is the reorganization energy.

reaction occurs by driving the reactants and the products in high-energy configurations, leading to a non-conservation of the energy. The idea by Marcus is related to the introduction of fluctuations in the energy due to the fluctuating configuration of the nuclei and the solvent molecules, both for the reactants and for the products. The

fluctuations could drive the overall system in a situation of intersection between the reactants and products energy curves. At the intersection, electron transfer can occur according to the Franck-Condon principle and satisfying energy conservation. If at the intersection point between the two curves the interaction between reactants is strong, a splitting of the curves occurs. In this case the system will remain in the lowest energy curve and the movement from products to reactants will occur adiabatically. In case of low interaction, the products will tend to remain on their curve also after the intersection point. The latter case can be described by a non-adiabatic treatment. In this case, considering the Arrhenius description for reactions and equation [1], the reaction rate will be given by:

$$k_{et} = A \exp(-(\Delta G_o + \lambda)^2/4\lambda RT) \quad [2]$$

As we will see in the following, the presence of two terms contributing to the reorganization energy could be relevant in

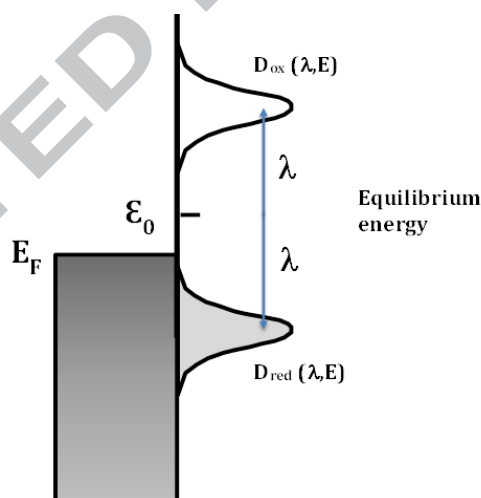


Figure 2: Gerischer formalism for describing the electron transfer mechanism in electrochemical experiments. The redox species is represented by the distribution of reduced ( $D_{red}(\lambda, E)$ ) and oxidized states ( $D_{ox}(\lambda, E)$ ). The equilibrium energy  $\epsilon_0$  is half-way between the maxima of the two distributions and the distance is the reorganization energy  $\lambda$ . The states on the metal electrodes are described by the Fermi energy level  $E_F$ .

reactions occurring in the EC-STM set-up, where the outer component could be affected by the presence of electrodes which could exclude part of the solvent.

According to the Marcus theory, the activation free energy has a quadratic dependence on the Gibbs free energy and the reorganization energy. A very important consequence of the Marcus theory is that, due to the dependence of the reaction rate on the combination of Gibbs free energy  $\Delta G_0$  and reorganization energy  $\lambda$ , a maximum rate will be reached for a specific value of the driving force which will be followed by an inversion region where, increasing the driving force, the reaction rate will decrease. This inverted region has been observed experimentally in many cases.

In proteins, electron transfer with cofactors could occur also at large distances (in the order of a few nanometers). In this case it is the protein itself which provides the medium for the electron transfer process to occur. The fact that the redox center is typically embedded in the protein matrix strongly reduces the outer sphere reorganization energy and the structure of the coordination environment around the redox center can also decrease the inner sphere energy. By using Ru-modified proteins (for example Azurin) it has been possible to change the tunneling distance between the redox center and Ru to study the role of the distance and the intervening medium on electron transfer rate. For azurin, an exponential dependence of the rate on the distance has been obtained with a decay constant of 0.11 nm suggesting a behavior for the protein medium similar to superexchange tunneling across saturated alkane bridges [26].

In the context of molecular electronics, electron transfer reactions occur between two metal electrodes in the presence of a voltage drop. As a consequence, the voltage drop inside the gap can alter the distribution of the energy levels in the molecule and the presence of the electrodes and any charge connected to the electrodes can modify the molecular orbitals. Moreover, the electron transport mechanism is also different from the mechanism usually involved in electrochemical experiments. In fact, electrochemical experiments involve the presence of only one solid electrode instead of two electrodes. In the case of electrochemical reactions performed at a metal surface, the driving force for oxidation or reduction of the molecule is provided by the energy difference between the electrode potential multiplied by  $e$  (the electron charge) and the energy corresponding to the equilibrium between the reduced and oxidized species (the energy corresponding to an equal concentration of oxidized and reduced molecules. Considering single molecules we will refer to the probability instead of the concentration). According to this situation, the activation energy for the reaction is given by a quadratic

dependence on the reorganization energy and the applied overpotential, as described by the Marcus theory. When electrons are exchanged with a metal electrode, it is important to consider also the density of states on the electrode itself, so the Fermi-Dirac distribution will play a role and the energy position of the electron in the metal should be considered. The electron exchange will be proportional to the integral performed on all the allowed energy levels, even if the integral will be negligible far from the Fermi level of the electrode. A very useful description of the situation in this case is provided by the Gerischer formulation [8, 27,28] which can be extended also to the EC-STM configuration. The basic idea of the Gerischer formulation of the Marcus theory is that electron transfer occurs between occupied and unoccupied states together with the fact that thermal fluctuations of the solvent induces a broadening of the redox energy levels. The total rate for electron transfer results from an integral over the states (or energies) which might be involved. If a metal electrode is involved, the energy levels which matters are given by the density of states around the Fermi level. For species in solution, the Marcus theory can be applied for the density of states. The exponential dependence of the reaction rate on the activation energy is considered. The Marcus theory foresees for the activation energy a square dependence on the free energy variation and this square dependence is reflected in a Gaussian shape for the density of reduced (occupied) or oxidized (empty) states in the molecule. The application of an overpotential to the metal has the equivalent effect of shifting the entire distribution of the density of states while leaving the set of states involved unaffected, independently of the specific value of the Fermi level (Figure 2). If the process is a reduction, the occupied state which is providing the electrons is on the electrode and the receiving state is on the electroactive species. In the opposite case of an oxidation, the occupied state providing the electron is on the redox species, and the receiving state is on the electrode. In the case of the presence of two electrodes in the proximity of the molecule, the potential difference between the two electrodes will be the driving force for the electron transfer from one electrode to the other by means of two electron transfer events, at least if the redox level is going to play a role in the transport mechanism.

## ECSTM as a configurable nanobiodevice

If one considers devices based on a single or a few molecules, the instrument of choice for the characterization of the transport properties through the proteins joining two metal electrodes is the Scanning Tunneling Microscope (STM) [29]. Since their advent, scanning probe microscopy techniques strongly prompted experiments in the field of molecular electronics. In the specific case of protein-based nanodevices, the operation in physiological environment could prevent problems connected with partial or total denaturation and could allow to fully exploit molecular redox properties by means of the control of solution potential. In this case the STM should be used in its electrochemical implementation [30]. Soon after the introduction of the STM working in air or in vacuum conditions, researchers attempted to operate it in liquids. Obviously, in such implementation, tunneling current flows in a conductive medium and Faradaic and capacitive currents might occur at the electrode surfaces. In order to control non-tunneling contributions to the overall current, the STM tip is coated everywhere but the apex by an insulating layer, which strongly limits its surface area exposed to the liquid medium. Moreover, the tip and the conductive substrate are typically connected to a bipotentiostat that allows controlling their potential with respect to a reference electrode in solution. This control is achieved by means of a fourth electrode, the counter electrode, which plays the role of sacrificial electrode (Figure 3). The potential applied to the metal electrodes allows to limit Faradaic currents to figures which are negligible with respect to the tunneling current set-point, making tunneling current the dominant one that flows between tip and substrate.

The presence of two working electrodes (tip and substrate) allows two different types of spectroscopic experiments to be performed by ECSTM. In one case, the substrate-tip bias voltage can be kept constant while their potentials can be varied with respect to the reference electrode. In this case the bias voltage, proportional to the Fermi level of the two working electrodes, can be rigidly shifted in order to include, inside its window, energy levels of the molecule(s) sandwiched between the two. Alternatively, the bias voltage can be swept according to the usual Scanning Tunneling Spectroscopy – STS – in which the potential of one electrode is fixed while the other is varied. The former case is usually referred to as Electrochemical Scanning Tunneling Spectroscopy (EC-STS).

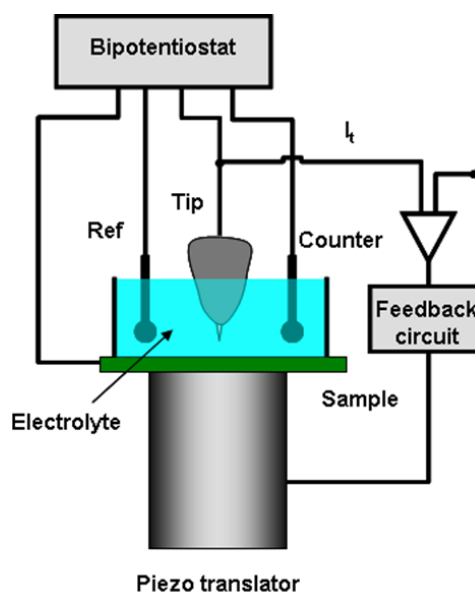


Figure 3: Schematic representation of an EC-STM set-up with bipotentiostatic control.  $I_t$  represents the tunnelling current that feeds the feedback system in constant current mode imaging.

This possibility is useful when the transport characteristics of a redox molecule are to be investigated. In fact, with the ECSTS technique it is possible to shift the two electrode Fermi levels in order to include the molecular energy levels (not pinned to any of the Fermi levels) inside their voltage window. In this configuration, the electrolytic medium can play the role of gate electrode in a usual FET configuration, where tip and substrate are source and drain electrodes, respectively [31]. By changing the electrochemical potential of the solution, the energy levels of the molecules can be involved in the electron transport mechanism between tip and substrate.

It has been shown that a sort of electrolyte gating can be achieved with several redox molecules [21,22,32-38]. This mechanism consists in an increase of the tunneling current flowing through the molecule for particular values of the electrolyte potential. By continuously changing the potential of the electrode on which the redox molecule is immobilized with respect to the reference electrode, while keeping the substrate-tip bias voltage constant, the tunneling current flowing through some redox molecules shows a resonance-like trend (increase of the tunneling current in a specific potential range followed by a decrease of the current) confirming the proof-of-concept of a single molecule transistor. In this case, the origin of the

gating mechanism is traced back to the solution potential affecting the energy position of the molecular levels (or, *vice versa*, the solution potential can be considered fixed and the Fermi levels of the two electrodes are varied).

This behavior is reminiscent of a field-effect transistor in the solid state. However, in spite of some similarities between solid-state, field-effect transistor and electrolyte-gated transistor, the physics behind their operating mechanism is quite different. Indeed, as it will be described in more details below, transport properties in an electrolyte-gated transistor involving one or a few redox molecules depend on so many parameters that different characteristics might be observed, conferring to a single device different functional properties (switch, transistor or negative differential resistance).

Many studies have investigated how the energy levels brought about by a redox molecule sandwiched between tip and substrate can be involved in the electron transport mechanism [39-42] (see below). It is important to consider that there are always two possible transport channels when considering a redox molecule filling the gap between an STM tip and a conductive substrate. One channel is due to the electronic coupling of the molecule with the electrodes and to the delocalization of the electrons in the orbitals. The second channel, which is characteristic of redox molecules, is due to the possible population of the redox levels by the electrons flowing between the two electrodes and the vibrational molecular relaxations coupled to the environment. A common feature in this context is a different conductance of the molecular species when stabilized in different redox levels. Typically, a strong variation of the molecular conductance upon different redox states confers on the system a switch-like behavior rather than a transistor-like one. Therefore, apart from a direct involvement of the vibrational relaxation of redox molecular levels and nuclear degrees of freedom, the electronic delocalization and coupling with the metal electrodes that could change according to the different redox state of the molecules, should be considered [43].

There can be different experimental configurations suitable to investigate transport properties by ECSTM. Initially, the different conductance of the molecules were established by acquiring a sequence of STM images of the same sample area with the same bias voltage but for different values of the substrate potential with respect to the reference electrode [32]. A variation of the apparent height, with respect to a reference, or a non-varying feature in the image, is considered as an indication of a different molecular conductance. Two

aspects of this experimental approach ought to be stressed. The first aspect is related to the fact that the real variation of the current as a function of the gate potential is not directly measured. The measured apparent height is connected to the tunneling current decay constant. The second one is due to the fact that the substrate/molecule/tip junction is not symmetric because the connection to the tip might not be of the same type as that to the substrate (see Figure 4). This configuration asymmetry can have specific effects on the measured current through the molecular junction.

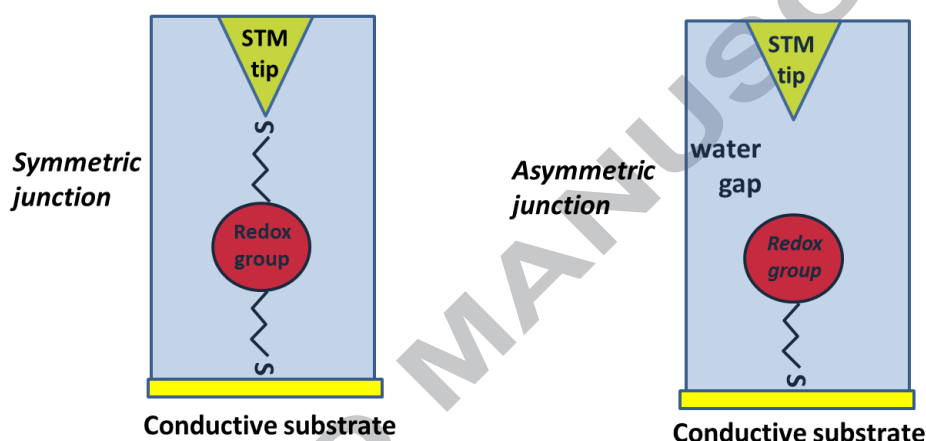


Figure 4: Possible configurations for a redox molecule in the gap between the conductive substrate and the STM tip in the EC-STM set-up.

Another possible experimental approach is that of immobilizing the molecules of interest on the substrate or on the tip, approaching the tip to the substrate until a defined current set-point is obtained and then equilibrating the tip-substrate distance by using the active feedback system [21]. Afterwards, the feedback system is switched off and the substrate or tip potential is varied with respect to the reference electrode while keeping constant the bias voltage. In this regime, the tunneling current is measured directly. Even using this method the transistor-like behavior of single redox molecules including redox proteins, has been observed [21].

Also in EC-STM, like in case of STM in air or vacuum, it is possible to perform the usual  $I-V_{\text{bias}}$  spectroscopy. In this case, particular attention should be paid to the presence of capacitive currents that can overwhelm the tunneling current of interest. At the same time, the  $I-V_{\text{bias}}$  curves can be measured for different values of the electrode potential.

Recently, the break-junction technique, which was introduced in the context of molecular electronics for measurements in air or in

vacuum, has been extended by Tao et al. to the STM set-up [44]. Here, the current flowing through a molecule is measured when it is covalently bonded both to tip and substrate during a withdrawing process of the STM from an initial position close to the substrate (see Figure 4). The attainment of tip/molecule contact is verified by the presence of a plateau in the plot of the tunneling current versus tip/substrate separation, followed by an abrupt jump. If the molecular construct is symmetric, this particular experimental configuration measures the tunneling current and the molecular conductance in a symmetric arrangement (differences might result from the geometry of the two electrodes and from the different materials used for the substrate and the tip). Many (thousands) repetitions of the measurement can be performed and the distribution of the values for the current plateau allows establishing the most probable value of the molecular conductance. These experiments can be performed for different values of bias voltage and, while keeping the bias constant, for different values of the electrode potentials. Using this approach, it is possible to reconstruct, by a sequence of points, the curves obtained with the previous approaches. Notably, this technique avoids problems connected with capacitive currents arising when sweeping bias voltage.

Moreover, in the case of a very stable junction, it is also possible to approach the tip to the substrate, to wait for the formation of a covalent bond between the tip and the free end of the molecule and then, after disabling feedback system, to perform a sweep of the electrode potential with respect to a reference [45]. In this approach a continuous monitoring of the spectroscopic data is performed with the molecule in a symmetric configuration.

### **Theories for ECSTM of redox molecules**

The EC-STM configuration can be theoretically described considering an electron transport phenomenon resulting from two electron transfer events. Each electron transfer process involves a metal electrode, the substrate and the tip, respectively. A particular case is obtained when the molecule sandwiched between the two electrodes is a redox molecule whose energy levels can be tuned by the reference electrode in solution. From a theoretical point of view the study of redox molecules in EC-STM configuration began in the early '90s with the works by Schmickler and Kutznesov and Ulstrup [46,47]. The chosen approaches relied mainly on the Gerischer

formulation of the Marcus theory that we described above. Depending on the degree of coupling of the molecule with the two electrodes, different scenarios were described for the overall transport phenomenon. In the case of weak coupling, the overall transport process of one electron between the two metal electrodes foresees two electron transfer steps. According to the initial position of the energy levels, a first step can occur from the substrate to the molecule, which subsequently relaxes to its reduced state, stabilized by the reorganization of the solvent. The positions of the energy levels fluctuate due to fluctuations of the coordinate of the vibrational mode. These fluctuations could bring the electron energy level to the region near the Fermi level of the second electrode where the second electron transitions can effectively occur, leaving the molecule again in its oxidized state. The stabilization of the electron on the molecule represents the prevalence of a hopping transport mechanism on a tunneling one in which the time of residence of an electron on the molecule is negligible and does not allow for reorganization of the molecule/solvent system. Between the two extreme situations of hopping and tunneling, many other cases could be given, by varying the degree of coupling between the molecule and electrodes. In the case of strong coupling, the first electron transfer can initially induce a partial relaxation of the molecule. While the energy level of the molecule is inside the window defined by the Fermi energy levels of substrate and tip, this represents an open channel for the transfer of a great number of electrons from the substrate to the tip (Figure 5a). The latter mechanism gives rise to a high transport current, which might be compatible with many experimental results so far obtained. An analytical description in the case of strong coupling is usually obtained by considering the electron transfer rates in the direction of the electron flow imposed by the bias voltage neglecting the inverse transitions. This relation is given by Equation 3 [48]:

$$I = e \kappa \rho(e E_{bias}) \frac{\omega}{2\pi} \left\{ \begin{array}{l} \exp \left[ \frac{e}{4\lambda kT} (\lambda + \xi \eta + \gamma E_{bias})^2 \right] + \\ \exp \left[ \frac{e}{4\lambda kT} (\lambda + E_{bias} - \xi \eta - \gamma E_{bias})^2 \right] \end{array} \right\}^{-1} \quad [3]$$

where  $\kappa$  is the electron transmission coefficient,  $\rho$  is the density of states in the electrodes near the Fermi energy,  $\omega$  is the characteristic nuclear vibration angular frequency,  $\eta$  is the overpotential (the difference between the Fermi level of the electrode and the

equilibrium level for the redox species),  $\xi$  and  $\gamma$  are two parameters which describe the potential profile inside the gap between the two electrodes (shift of the bias voltage and overpotential, see Figure 5b for an explanation of their meaning) and  $E_{\text{bias}}$  is the imposed bias voltage.

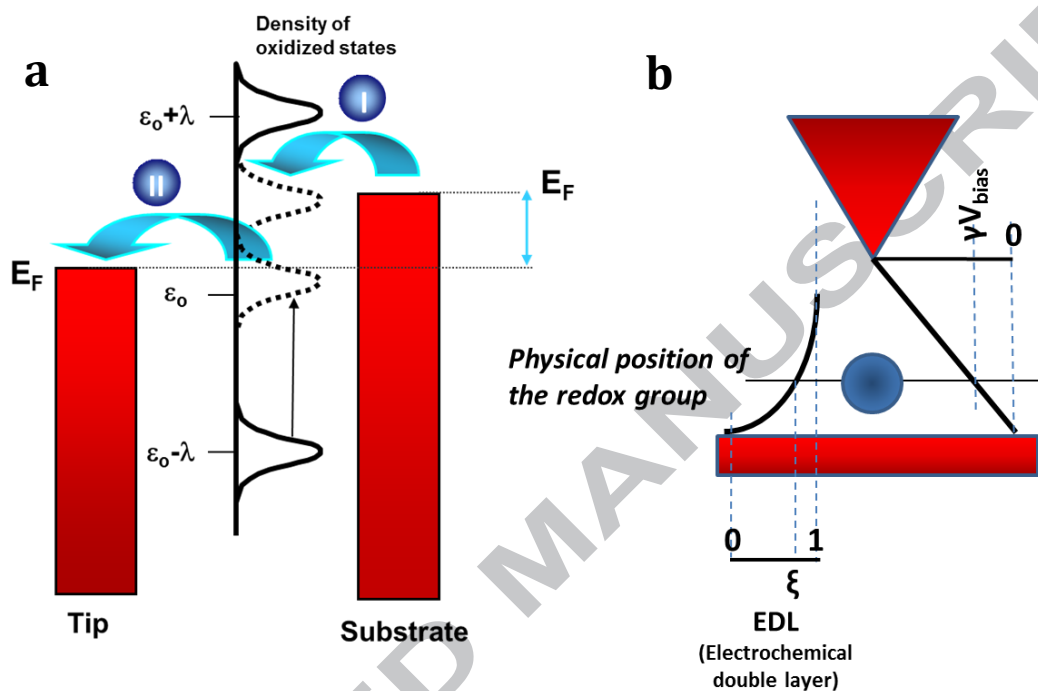


Figure 5: a) Schematic representation of the energy bands in the sequential two-step electron transport model; b) scheme of the potential drops inside the tunneling junction in the EC-STM configuration.

This description foresees the possibility of an electrochemical gating effect related to specific values of the substrate potential providing a maximum for the tunneling current. In particular, the maximum is obtained for values of the substrate potential near the equilibrium value of the redox species.

For redox molecules we have also to consider that the stabilization of a specific conformation of the redox molecule (oxidized or reduced) can by itself give rise to an increased or decreased efficiency for the transport of electrons between the tip and the substrate. The latter effect is the result of a variation of the delocalized orbitals in the molecule. This means that, for example, a reduced state of a molecule can give rise to more delocalized orbitals, which assure a more efficient conduction with respect to the oxidized state. Taken by itself, this phenomenon can imply an electrochemically controlled switching behavior of the molecule. Considering both the electrochemical gating

effect and the switching behavior, two conduction channels might be present in the case of redox molecules: a first channel related to the temporary population of the redox level of the molecule and a second channel related to the delocalization of electrons in the molecule according to the redox state of the molecule itself [43]. Altogether, these phenomena can give rise to a variety of non-linear behaviors of the tunneling current through redox molecules.

The first experimental evidence of the electrochemical gating effect was provided by Tao in 1996, when he showed that, by keeping the bias voltage constant, the tunneling current through Fe-porphyrins was strongly dependent on the potential of the substrate on which they were adsorbed. This behavior, schematically reproduced in Figure 6a, resembles that of a single-molecule transistor and it has a strong relevance in the context of developing a nanodevice. After this experiment, many other experimental evidences of a transistor-like effect have been obtained for different redox molecules, such as, for example, viologen [34,48], carotenes [49], transition metal complexes [35], derivatives of redox co-factors (e.g., quinones with thio-alkyl chains) [36,37,50] and metalloproteins [51-53]. The experiment by Tao, like many other experiments that followed, was based on repetitive imaging of the same sample area with constant tip/substrate bias but with different substrate potential values. This kind of EC-STM experiments relies on the measurement of the change in apparent height of the molecular features in the images, which is strictly related, but not easily understandable in a quantitative way, to the decay factor of the overall transport phenomenon in the tunneling gap. Moreover, the configuration of the studied molecular species is necessarily asymmetric due to the different interactions it establishes with tip and substrate. The water gap could be formed on the substrate or tip side. This asymmetric situation implies that the current measured in the EC-STM configuration does not allow measuring the single molecule conductance, rather, the conductance of the overall gap. Apart from the continuous scanning of the same sample area for different values of substrate potential with respect to the reference electrode, it is possible to perform spectroscopy measurements without lateral scanning of the EC-STM tip. In this case the tip is brought near to the molecule until a given current set-point is reached (or, in a reversed configuration, the molecules adsorbed at the tip surface are brought near to the substrate). Then, the z-feedback mechanism is switched off and, in the case of sufficiently stable tunneling gaps, the substrate potential or the tip/substrate bias potential are changed while measuring the

corresponding tunneling current at constant distance. It is also possible to directly access the single molecule conductance by exploiting a symmetric configuration in which a molecule is transiently bound in a covalent way to both the substrate and the tip. This configuration has been obtained by exploiting the STM break-junction technique developed by Tao. Here, the current through the molecule is measured during a withdrawing process of the STM tip from an initial position near to the substrate. This procedure allows measure the current through the molecule as a function of the substrate potential and of the molecular oxidation state. The break-junction configuration is easily implemented for certain type of molecules, whereas is more problematic in the case of single proteins, even if some studies have been performed for proteins (see below). The tunneling properties obtained for molecules bound to both electrodes might be different from the transport properties measured for the same molecules in asymmetric configuration. Indeed, in some cases, tunneling current showed a clear resonance in asymmetric junctions whereas the transport properties for the same molecular type in a symmetric junction showed a sigmoidal behavior characterized by a growth of the conductance across the region where the molecule changed its oxidation state which is not followed by a decrease of the conductance. This behavior has been attributed to a so-called “soft gating” mechanism related to the different configuration fluctuations allowed to the molecule in the two experimental set-ups [34,54,55]. However, in other cases, even in symmetrical configuration, a resonance-like behavior has been found. As already stated, the current measured through redox molecules as a function of the electrochemical potential of the solution might involve both an electronic restructuring and a contribution of molecular and solvent fluctuations around the different redox states. The first contribution, which can be assimilated to an inner sphere contribution to the current, typically gives rise to a sigmoidal trend of the current (represented in Figure 6b) as the redox state of the molecule is changed. The second contribution is more related to solvent fluctuations and coupling of electrons to vibrational effects and typically gives rise to resonance-like features in the tunneling current. Depending on which of the two contributions is more relevant, the tunneling current across a redox molecule will display either features. The two contributions can be present together at the same time. In this case the sigmoidal behavior of the current will be superimposed to the resonance-like behavior like in the trace represented in Figure 6c.

Recently, the interpretation of ECSTM experiments, especially the asymmetric ones on redox metalloproteins, based on the 2-step ET mechanism with partial vibrational relaxation has been questioned [56] in favor of another model: the Newns–Anderson model for electron transport in the case of solvent and intramolecular reorganization [57-59]. This model is typically used to describe chemisorption of molecules on metal electrodes by the introduction of an Hamiltonian and the formation of projected density of states for the adsorbate. The molecular junction is modeled as a single energy level interacting with two electrodes which in the context of EC-STM are the tip and the substrate. The molecular orbital is then coupled to vibrational modes occurring during the charge transfer event. The inadequacy of the 2-step ET mechanism was suggested considering mainly its inability to quantitatively reproduce the values of the tunneling current obtained in experiments on metalloproteins and the typical value for the redox equilibrium value exploited to fit the data. Moreover, using the 2-step ET framework, different experiments on the same metalloprotein azurin required different values for the parameters to fit the data, whereas the alternative model allowed interpreting quantitatively different experiments using very similar parameter values. This model stresses the importance of the real value of the molecular redox equilibrium value in the specific EC-STM set-up. It also stresses the asymmetry of the junction when experiments are not performed in the break-junction configuration and the strongly reduced value of the reorganization energy. These considerations have been prompted by transition voltage experiments performed in the EC-STM set-up by Artes et al. [60] and they suggest that the application of this technique to EC-STM experiments on redox molecules will provide new insights on the details of the electron transport mechanism.

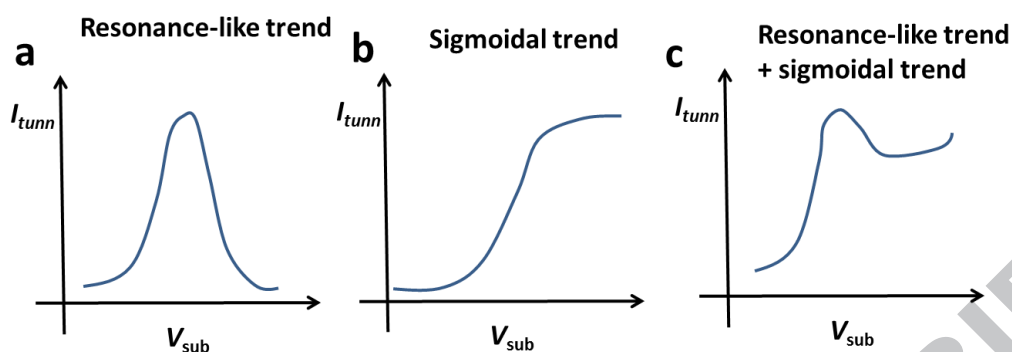


Figure 6: Different behaviors for the tunneling current through the junction between the tip and the substrate of an EC-STM set-up which includes a redox molecule gap. a) resonant-like behavior typical of the electrochemical gated process; b) sigmoidal trend mainly due to a different conductance of a redox molecule in the two different configurations (oxidized and reduced); c) overlap of the two trends.

### EC-STM of redox metalloproteins

Redox or electron transfer metalloproteins are endowed with one or more metal ions in their active site. The oxidation state of the active site can change reversibly, providing the possibility to exchange electrons with other biomolecular partners and contributing to many fundamental processes for life. The metalloproteins can be classified mainly in three families: blue copper proteins (or cuprodoxins), cytochromes (containing heme groups) and iron-sulfur complexes; moreover, one can add the chlorophyll-based photosynthetic complexes (e.g. reaction centers, antenna complexes) that are redox metalloproteins where an electron transfer cascade is induced by a preceding photoionization process [11]. The many studies directed towards metalloprotein characterization have provided a deep understanding of the structure and function of several of these redox molecules and they have shed light on the mechanisms used by some of these biomolecules to exchange electrons between molecular partners.

### Azurin as a model system

The "blue copper" metalloproteins comprise redox biomolecules bearing a single Cu ion in their active site, characterized

by a distorted co-ordination geometry that causes their typical intense blue color. Blue-copper proteins are usually involved in some of the early steps of respiration and photosynthesis [61]. Their family is mainly comprised of azurin, plastocyanin, amicyanin, rusticyanin, caeruloplasmin. In the context of EC-STM, azurin has been thoroughly investigated due to a series of peculiar features and it can be considered a model system. Accordingly, in the following we will describe some of its main peculiarities.

Azurin from *Pseudomonas aeruginosa* is a water soluble, relatively small protein (molecular mass 14600) [62]. Its functional role has not been established yet with certainty but most likely is that of soluble electron carrier. *In vitro* studies have shown that azurin can react with several redox proteins such as cytochrome  $c_{551}$  and ethanol dehydrogenases [63] and other dehydrogenases in different bacteria. Furthermore, azurin can donate or accept electrons to/from nitrite reductase, that is, however, not its physiological partner. Azurin's *in vivo* electron transfer activity appears to be related rather to cellular response to redox stress, hence suggesting cytochrome *c* peroxidase as a possible physiological partner. From a redox chemistry point of view, azurin functional behavior depends on the reversible oxidation of  $\text{Cu}^{1+}$  to  $\text{Cu}^{2+}$ . Peculiar electronic properties are connected to the special structural features of its redox site. Indeed, it is formed by a copper ion ligated to two histidines (His46 and His117) and a cysteine (Cys112), strongly bound to copper. The S atom of Met121 and the main chain carbonyl oxygen of Gly45 complete the trigonal-bipyramidal coordination geometry of the copper site of the wild type protein. The resulting geometry provides an intense optical absorption band at 628 nm and a small hyperfine splitting in the electron paramagnetic spectrum. For the same reason, azurin is endowed with a surprisingly large standard potential (+ 116 mV vs SCE) [64] in comparison to that of the  $\text{Cu}(\text{II}/\text{I})$  aqua redox couple (-89 mV vs SCE). Molecular structure has a globular shape characterized by mainly a  $\beta$ -barrel conformation, figure 7. The active site is buried inside the molecule and appears located  $\approx 0.8$  nm underneath the globule surface; it features also an exposed S-S bridge that is formed by the thiol moieties of Cys3 and Cys26 side chains. The last features are particularly relevant in the context of EC-STM experiments on this molecule.

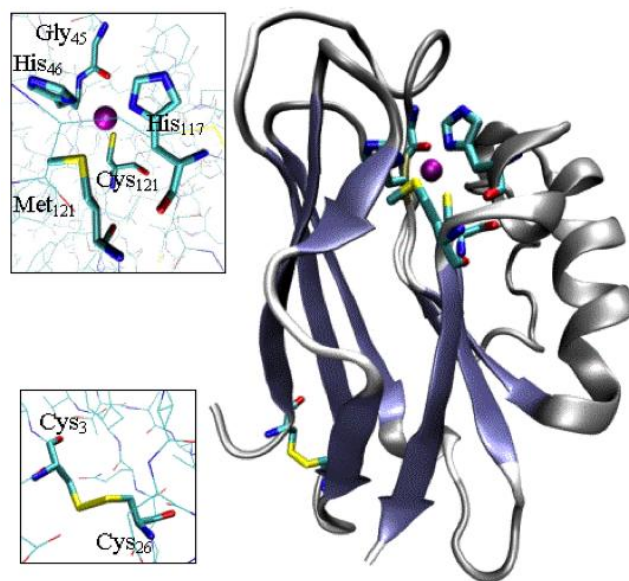


Figure 7. Schematic representation of the structure of azurin from *Pseudomonas aeruginosa*. Note the Cu ion represented as a dot in the upper part of the structure; in the insets, the active site and the disulphide bridge are highlighted. Structural information from PDB file 4AZU [65].

Indeed, the presence of an exposed disulfide provides a very convenient anchoring point to chemisorb azurin at the surface of metals such as Au, Ag, Pt, Cu, etc. by reduction of the bond and the formation of one or two Me-S bonds. Moreover, its  $\beta$ -barrel conformation provides the protein with a remarkable resistance to the mechanical action of the scanning probe, particularly useful in case of repeated scans.

### EC-STM experiments on metalloproteins

The first evidence of potential dependent EC-STM contrast on a metalloprotein was performed on azurin which was chemisorbed on Au(111) substrates [53]. EC-STM imaging showed features emerging from the terraces of the Au(111) film. The imaged structures were ascribed to single azurin molecules immobilized on the gold surface. The typical bright spots, which were repeatedly imaged by the spectroscopy-like imaging procedure while keeping the substrate/tip

voltage constant, showed an apparent height with respect to the gold substrate that was strongly dependent on the substrate potential which was controlled with respect to the reference electrode. A further experiment confirmed the role of the metal redox-active site in determining the height of the features with respect to the substrate [52]. This aspect was verified when azurin molecules bearing a Zn ion instead of Cu in the active site were mixed with the usual Cu-azurin. The internal control of the experiment was provided by the fact that Zn is not electro-active in the explored potential window. Upon substrate potential variation, some of the proteins varied their apparent height while others remained unchanged (Figure 8). Being the percentage of varying vs non-varying spots equal to that of the Cu vs Zn azurin molecules, the varying ones were attributed to Cu-azurin, also considering the previous investigations. The analysis of a single contrast-varying spot, based on its apparent height with respect to non-varying ones highlights a resonance-like behavior with its maximum at  $-0.21$  V vs SCE (Figure 8h). As we discussed in the theoretical section, the position of the current maximum provides, in principle, a criterion to shed light on the involved electron transfer mechanism. Considering the possible electron transport mechanisms in this context, it has been established that the mechanism at play in this kind of experiments is the two steps one with a partial vibrational relaxation and partial coherence

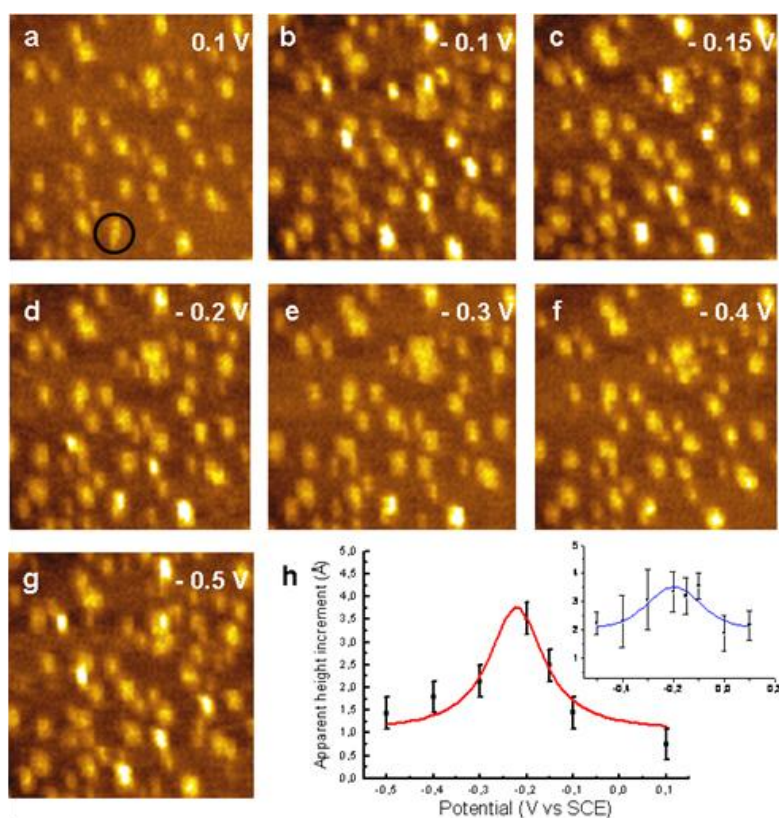


Figure 8: (a)-(g) EC-STM spectroscopy-like-imaging of a mixture of Cu- and Zn-azurin molecules adsorbed on a Au(111) substrate [52]. The value of the substrate potential with respect to SCE is reported in each image. Some molecules do not change their apparent height upon substrate potential, at variance with others. In (h) the apparent height increment of a spot (in the black circle in a) with respect to the non-varying ones is reported. The inset to (h) reports the apparent height increment averaged over six molecules. (Other imaging conditions: tunnelling current set-point 1 nA, bias 400 mV tip positive, scan range  $130 \times 130 \text{ nm}^2$ ).

As we already noted in the experimental section, by accessing directly the tunneling current instead of the apparent height, it is possible to gain more insights into the transport mechanisms. In order to obtain a direct access to the current it is possible to exploit a different experimental configuration. Azurin molecules have been chemisorbed on an EC-STM gold tip facing a Au (111) substrate [21]. In this set-up, the gold tip is then brought within tunneling distance from the gold substrate and the overall junction is stabilized at a set-point tunneling current of about 100 pA. By switching off the feedback and sweeping the tip potential at constant bias it is possible to measure the current flowing through the junction. This configuration allows investigating directly the tunneling current dependence upon

tip potential for different values of the bias voltage. The tunneling current between the tip and the substrate through azurin as a function of tip potential showed a clear current maximum, presumably due to temporary population of azurin redox states aligned with the Fermi levels of the gold electrodes of both the tip and the substrate. It is to be stressed that the measured current maximum was reproducible and reversible, assuring that the experimental configuration didn't induce irreversible structural modifications of azurin. The effect of the bias voltage on the tunneling current was studied showing that the current maximum and the width of the curve increased with bias, while the position of the maximum shifted to positive tip potential values (Figure 9). This specific experiment was recently exploited to show that alternative model with respect to the usual 2-step ET mechanism can be used to interpret EC-STM experiments on redox metalloproteins [56]. The behavior of the tunneling current in this experiment allowed getting insight into some theoretical aspects of the electron transfer mechanism. In particular, the experimental  $I$ - $V_{\text{tip}}$  results for different tip-substrate bias voltage are reported in Figure 9.

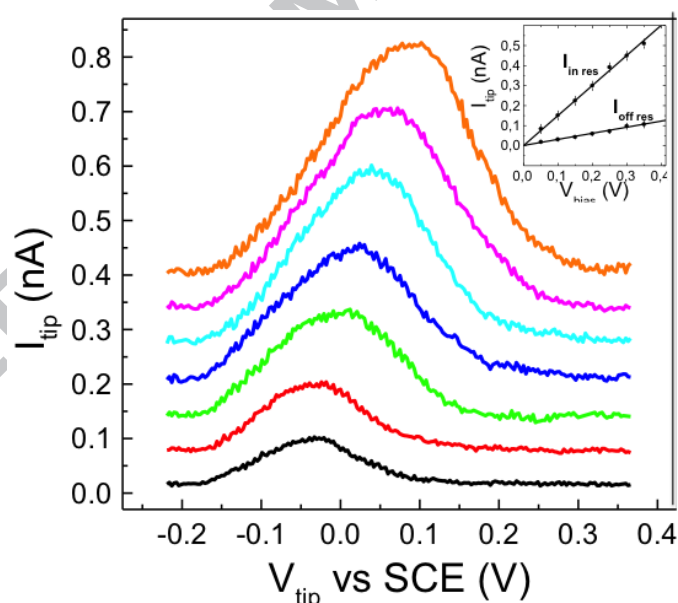


Figure 9: Bias voltage dependence of the trans-characteristics. Curves (displayed with an offset of 50 pA each to avoid overlap) were obtained at different bias voltage stepped by 0.05 V in the range 0.05 ÷ 0.35 V, starting from the lowest curve using a sweep rate of 2.4 V/s. Inset:  $I_{\text{tip}}$ - $V_{\text{bias}}$  characteristics measured from the set of curves at  $V_{\text{tip}} = -0.2$  V ("off res") and at each current maximum position ("in res"), showing a different tunnelling barrier transparency [21].

The STM break-junction technique has been applied also in the case of single metalloproteins. This technique, as we already noted in

the description of the experimental set-ups, allows determining the single molecule conductance. Moreover, the technique allows studying the transport properties of proteins along different pathways, according to the specific groups chosen for establishing the contacts between the protein and the two electrodes. In this case, site-directed mutagenesis is typically exploited to introduce thiol functionalities which allow the formation of covalent contacts. By exploiting approaches of this type it is possible to study, in the context of the construction of a protein transistor, the best choice for contacts between the source and the drain electrodes. In an electrochemical environment, the STM break-junction approach has been applied to study the gating mechanism in azurin, even if the coupling of the electrodes to the protein was based on only one thiol bond) [66]. In fact, the second covalent bond is presumably based on an exposed lysine residue. In this study, the electrolyte gating effect has been found for the single azurin molecule conductance with a 20-fold on-off ratio, confirming previously acquired data exploiting constant-current EC-STM imaging and EC- Scanning Tunneling Spectroscopy.

An important aspect of single protein conductance in the ECSTM junction is the intrinsic flickering feature [67]. This behavior points to critical considerations in the context of single molecule devices. Indeed, a compromise between the stochastic behavior of single molecules and a few-molecules-averaged performance should be looked for in nanobiodevices to obtain more predictable results.

In the framework of redox metalloproteins, cytochrome *c* is one of the most studied molecules. Efforts to study this molecule by EC-STM imaging has already been performed, concentrating on cytochrome *c* from *Saccharomyces cerevisiae* (YCC) immobilized on Au(111) substrates [68]. A major concern in ECSTM experiments on metalloproteins is that of exploiting an immobilization strategy which allows preserving the protein redox functionality. This is particularly critical for YCC whose secondary structure is rich mainly in  $\alpha$ -helices [64]. ECSTM imaging of YCC exploiting an immobilization strategy on bare gold which largely prevents protein denaturation [69] maintaining the redox functionality has been performed. YCC was immobilized on gold by exploiting the C102 residue while keeping the protein in the reduced form. Under these circumstances, the immobilized protein layer is still electrochemically active with a very fast interfacial electron transfer to the substrate. Taking images of the immobilized proteins for different values of the substrate potential, different apparent heights have been measured, confirming the electrolyte gating effect also for cytochrome *c*.

Recently, an EC-STM experiment on a different type of cytochrome (cytochrome  $b_{562}$ ) modified in order to allow an easy immobilization on a gold surface, demonstrated the electrochemical gating effect with a resonance-like behavior for the tunnelling current as a function of the substrate overpotential (the difference between the applied potential and the equilibrium potential for the redox species) [70]. In another study, the orientation dependent conductance of cytochrome was studied by introducing pairs of cysteine residues that assure from one side the immobilization on the gold substrate and from the other side the formation of transient covalent bond with the STM tip [71]. By using the break junction technique the protein conductance through the long and the short axis was measured. The results highlighted that the placement of the asymmetrically located heme within the protein might influences electron transport process.

### **Other examples of nanobiodevices**

The data retrieved from surface-immobilized redox metalloproteins by Scanning Probe techniques operated in electrochemical environment, suggest clearly that these molecules behave like molecular switches, enabling or preventing electron flow through them according to the availability of molecular electronic levels in the energetic window comprised between the Fermi levels of tip and substrate. The possibility of switching the conduction state of an object such as a molecule by gating the flow of electrons through it, represents indeed the basic feature of a molecular (nano)transistor. Therefore, the idea of trying to implement a self-standing, single (few) molecule(s) transistor exploiting the electron conduction properties of metalloproteins (e.g. azurin) arises naturally [71]. Redox metalloproteins arranged in one-molecule-thick film in the gap defined by a pair of planar electrodes could hence act as the channel of a field-effect three terminals transistor. Of course, the problems posed by the implementation of such kind of devices appear immediately very serious and abundant. Among them, it is worth recalling two of them: i) the implementation and theoretical description of effective electrical contacts between metalloproteins and metal electrodes, and ii) the understanding and optimization of the mechanisms and conditions of intermolecular electron transfer in 2D ensembles of metalloproteins, including the fact that many of these devices are implemented in dry conditions. Here, we will not discuss

in details the requirements for the construction of these devices, i.e. the strategies for protein immobilization on a surface. We redirect the reader interested in this topic to reviews in the literature [72-74]. Even if a final solution for these problems is still lacking, the practical realization of working devices is possible and it has been accomplished in facts. Indeed, it has been found that proteins in dry environment have an electronic conductivity comparable to that of conjugated molecules, highlighting the fact that proteins offer a very efficient medium for electron transport. Typically, one can assume that electron transport between two electrodes separated by a monomolecular protein layer has an exponential dependence on the tunnelling barrier width (the thickness of the protein layer can be considered a good approximation for the barrier width). The decay constant can be taken as a signature of the type of transport mechanism, specifically to distinguish between superexchange and hopping mechanism [75]. Indeed, in principle it is possible to distinguish between a direct non-resonant tunnelling and a multistep tunnelling process [76]. It is also plausible that these devices could provide information on the basic transfer properties of proteins even if they are operated in an environment different from proteins' natural one.

The implementation of a FET - or single particle transistor-like protein device, should likely take advantage of state-of-the-art lithographic techniques for the definition of planar (nano)electrodes. Figure 10 depicts the operating principle of a generic single metalloprotein planar transistor. Here, a redox metalloprotein is placed in the nanometre-sized gap between two planar electrodes and is electrostatically coupled to a gate electrode. The coupling is responsible for shifting the electronic levels of the molecule with respect to the Fermi levels of the metal leads, enabling or hindering the electronic flow via the aforementioned levels. In this case, the choice of using metalloproteins is related to the possibility of exploiting energy levels that are specific for redox molecules. The idea is to use the typical features observed in electrochemical experiments on these molecules to perform a task in the context of solid-state electronics.

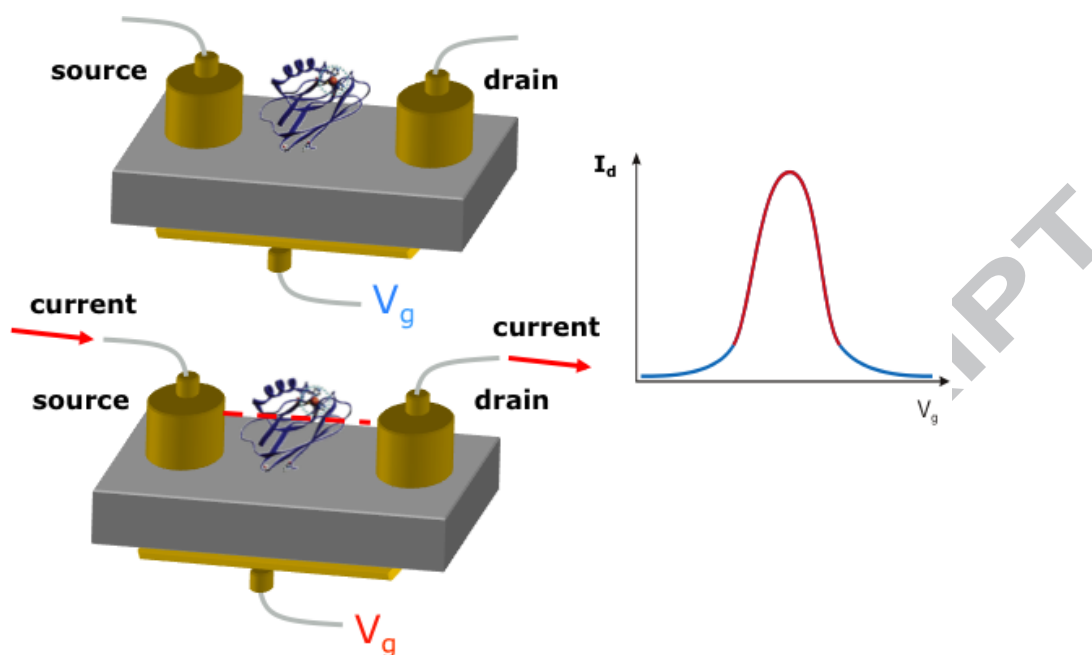


Figure 10: Scheme of a single metalloprotein planar nanotransistor. The gate electrode acts on the electronic levels brought about by the protein. When these levels are tuned to the Fermi levels of the leads, conduction via the molecule is enabled, bottom-left and right panel.

To date, a limited number of different planar nanobioelectronic devices have been realized. Typically, these make use of the redox metalloproteins that have so far shown the most robust performances as to withstanding large electric fields without undergoing denaturation and to survive rather non-physiological environments such as that of the surface of a hybrid electronic device.

The implementations reported so far have been those of two- and three-terminal devices; they have shown the feasibility of such hybrid devices and have been used especially to characterize those particular systems, trying to clarify the role of molecular organization and that of the particular metal ion in the protein.

The first implementation of a hybrid nanoelectronic device was that of a solid state molecular rectifier based on a (sub)monolayer of azurin molecules [77]. In this case, the main interest was in the protein layer transport properties. A monomolecular carpet of metalloproteins was chemisorbed on the surface of thermally grown  $\text{SiO}_2$  in between two gold nanoelectrodes (Cr-Au) defined by e-beam lithography (EBL). Protein chemisorption was achieved by a silane-based chemistry. The construct guaranteed a covalent linkage of the molecules to the surface as well as a defined, uniform orientation of the proteins on it. Control experiments on hybrid devices based on non-uniformly oriented azurin were performed using a different

immobilization strategy. Obtaining an uniformly oriented protein film in between nanoelectrodes is of extreme importance for the performance of an hybrid device for two main reasons: i) uniform orientation enables a higher surface coverage which can facilitate intermolecular electron transfer between neighbor metalloproteins; ii) for a given protein coverage, it endows the molecular carpet with a uniformity in the location and orientation of the Cu-based redox active sites, thus increasing electron transfer probability. Another important aspect, strictly related to protein orientation at surfaces, is protein electrostatics. Proteins, being zwitterionic molecules, possess on their surface a variety of charged and polar groups whose global effect is described by MEPs (Molecular Electrostatic Potentials). MEPs play a major role in protein-protein interaction and bio-recognition in solution and drive the phenomena of self-assembling at surfaces, as well as adsorption kinetics. MEPs for azurin have been computed in a number of different conditions involving different protein oxidation states, as well as solution pH, and ionic strength. Calculations have shown that azurin, in the experimental conditions used in the work at issue, possesses a strong dipolar moment (150 D) that can sum-up in an oriented, 2D molecular assembly, influencing the overall field sensed by electrons flowing in mono-molecular layer [77].

The electrical characterization of a two-electrode device with a gap of 60 nm is reported in Figure 11 for the uniformly, and randomly oriented protein edifices [77]. Some important features and differences are evident: i) the uniformly oriented sample shows a marked rectifying behavior (rectification ratio of 175 at 1.5 V vs a figure of just 10 for the randomly oriented counterpart); ii) the uniformly oriented sample shows a ten-fold higher current with respect to the randomly oriented one; this effect, along with that of rectification, can be traced back to the molecular dipoles summing-up in the self-assembled layer and providing an electrostatic field superimposing to the external one; iii) marked steps in the I-V curves, tentatively ascribable to the involvement in the conduction mechanism of protein redox levels, are present in both samples albeit different in intensity. This first demonstration of a metalloprotein-based molecular rectifier showed limited stability to aging and to environmental conditions, nevertheless suggesting that the essence of the observed phenomena was due to the presence of the molecules.

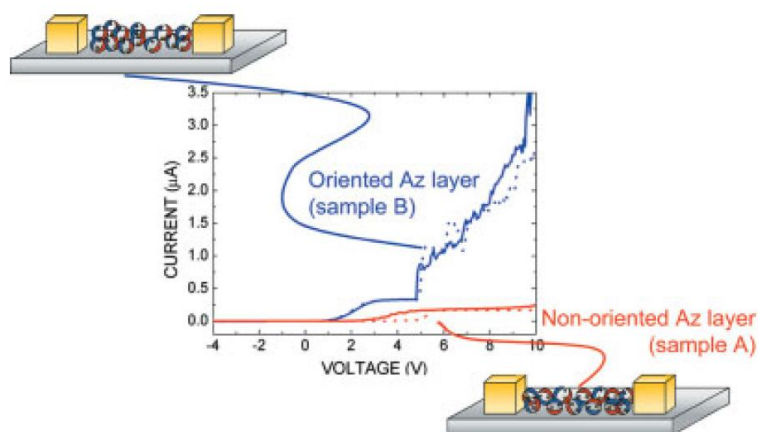


Figure 11: Current-voltage characterization for the randomly oriented Azurin sample (sample A) and for the uniformly oriented Azurin sample (sample B) in a 70 nm gap. Schemes of the possible orientation of Azurin molecules in the two configurations are shown [77].

A further work addressed several issues related to protein sample purity, and the role of the Cu ion in azurin active site [78]. In 50 to 100 nm wide nanogaps, it turned out that recombinant native azurin performed better than the wild type counterpart showing a rectifying ratio of 500 at 10 V. Moreover, an extensive study involving different molecules (recombinant native, Zn-azurin, and Apo-azurin – without the metal ion), all immobilized with a uniform orientation, was undertaken in order to understand the role of the particular metal ion in the active site, similarly to previous EC-STM studies at the level of single molecule. These results confirmed the key role of Cu ion and that of the electronic levels brought about by its presence, in assisting current flow through the molecular layer. Zn-azurin and Apo-azurin, albeit almost identical to Cu-azurin in molecular conformation, were in fact unable to elicit any appreciable current flow. Finally, the role of relative humidity in preserving the performances of the hybrid device over time was assessed. A relative humidity around 50% was found to be optimal for device performance and long-term operation.

As a further step, a three-electrode device was implemented [79], i.e. a device where the current through a molecular layer was controlled by a gate electrode in a FET-like implementation. In this case, attention was paid to the possibility of finding features in the electron transport phenomenon that could resemble the transistor-like effect identified in EC-STM experiments and related to protein redox properties. The experimental configuration for such a device was pretty much similar to the two-electrode one (EBL defined Cr/Au

arrow-shaped nanoelectrodes facing in a 100 nm gap on a Si/SiO<sub>2</sub> substrate). However, the main difference was the presence of an Ag electrode on the back of the structure, assuring an ohmic contact with the p-doped Si substrate. This electrode was used as gate in a FET configuration. The main results of this work were the presence of a marked resonance in the device trans-characteristics, Figure 12, which displayed a peak-to-valley ratio of 2 at  $V_g = 1.25$  V. Only devices assembled from Cu-azurin displayed such a feature, at variance with Zn- and apo-azurin.

Interestingly, the switching behavior of this protein-based FET was also modelled in a simplified frame of protein chains of alternating reduced and oxidized molecules, invoking a hopping mechanism for intermolecular electron transfer. Within that model, it was possible to account for the main experimental features of the implemented device, namely: i) the appearance of the described resonance in trans-characteristics (source-drain current vs gate voltage), and ii) the marked onset in the I-V curves, as already described in the implementation of the two-terminal devices.

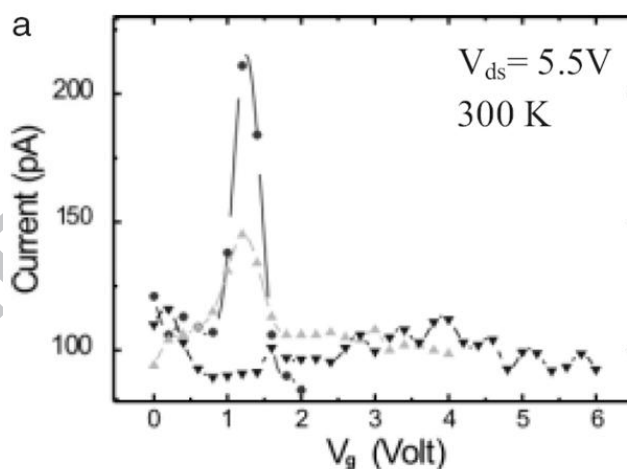


Figure 12: Three trans-characteristics (source-drain current vs gate voltage) obtained in temporal sequence (black circles, light grey triangles and black inverted triangles) on a 100 nm gap with Azurin molecules immobilized in a uniform orientation. In the resonance region, the trans-conductance changes from positive to negative values. The resonance feature gradually disappears [79].

Recently, Richter et al. developed a vertical transistor configuration based on a small channel in which proteins are located [80]. In this configuration, a central gate electrode is exploited to activate a self-assembled monolayer of proteins sandwiched between two metal electrodes playing the role of drain and source electrodes. It is to be stressed that, in contrast to the previously described planar

devices, in this configuration the current flow is in the same direction of the main axis of the self-assembled proteins, whereas in the previous case the current was perpendicular to the main axes. Furthermore, in the set-up by Richter et al., the current is measured over a very small monolayer area. As a consequence, in the previous set-ups the intermolecular electron transport mechanism has a relevance, which is not present in the last one, where the main transport occurs across one-protein layer. It has been shown that the gate potential is able to align the energy levels of the proteins inside the window defined by the Fermi levels of source and drain. By this technique it has been possible to ascertain the connection between the redox properties of the proteins and the presence of a Negative Differential Resistance feature in the I-V curves [81]. Once again, azurin has been used to perform this experiment and the results have been compared to the case of the apo-Azurin. The absence of any NDR peak in the case of apo-AZ suggests that the observed feature is related to the redox center of Azurin.

## References

- [1] J.-W. Choi, Y. S. Nam, and M. Fujihira, Nanoscale fabrication of biomolecular layer and its application to biodevices, *Biotechnol. Bioprocess Eng.* 9 (2004) 76-85.
- [2] E. Juanola-Feliu, P. Ll. Miribel-Català, C. P. Avilés, J. Colomer-Farrarons, M. González-Piñero and J. Samitier Design of a Customized Multipurpose Nano-Enabled Implantable System for In-Vivo Theranostics, *Sensors* 14 (2014) 19275-19306.
- [3] V. Rai, S. Acharya, and N. Dey, Implications of Nanobiosensors in Agriculture, *J. Biomater. Nanobiotechnol.* (2012) 18992.
- [4] M. J. Heller, and A. Guttman, *Integrated Microfabricated Biodevices: Advanced Technologies for Genomics, Drug Discovery, Bioanalysis, and Clinical Diagnostics* Marcel Dekker, New York, Basel 2002.
- [5] Y. Shinozaki, K. Sumitomo, A. Tanaka, N. Kasai K. Torimitsu, Examination of Ion Channel Protein Orientation in Supported Lipid Bilayers, *Applied Physics Express* 4 (2011) 107001.
- [6] P. Facci *Biomolecular Electronics: electrical control of biological systems and reactions*, Elsevier, New York, 2014
- [7] R. M. Iost, W. C. da Silva, J. M. Madurro, A. G. Madurro, L. F. Ferreira, F. N. Crespilho, Recent advances in nano-based electrochemical biosensors: application in diagnosis and monitoring of diseases, *Front. Biosci.* 3 (2011) 663-689.
- [8] A. J. Bard, L. R. Faulkner, *Electrochemical methods: Fundamentals and Applications*, 2nd Edition, John Wiley and Sons Inc., New York, 2001.
- [9] A. W. Bott, Redox Properties of Electron Transfer Metalloproteins, *Curr. Sep.* 18 (1999) 47-54.
- [10] G. I. Likhtenshtein, *Chemical Physics of Redox Metalloenzyme Catalysis*, Springer, 1988.
- [11] D. Devault, *Quantum-mechanical tunneling in biological systems* 2nd edition, Cambridge University Press, 1981
- [12] B. Alberts, A. Johnson, J. Lewis, D. Morgan, M. Raff, K. Roberts, P. Walter, *Molecular Biology of the Cell*, 6th edition, Garland Science, 2014.
- [13] A. Alessandrini, P. Facci, Electrochemically Assisted Scanning Probe Microscopy: a Powerful Tool in Nano(Bio)Science, V. Erokhin, M.K. Ram, O. Yavuz (Eds.), in *The New Frontiers of Organic and Composite Nanotechnology*, Elsevier, 2008, pp. 237-286.

- [14] L. A. Giannuzzi, F. A. Stevie, Introduction to Focused Ion Beams: Instrumentation, Theory, Techniques and Practice (Eds.), Springer, 2006.
- [15] R.F.W. Pease, Electron beam lithography, *Contemp. Phys.* 22 (2006) 265-290.
- [16] J. R. Arthur, Molecular beam epitaxy, *Surf. Sci.* 500 (2002) 189-217.
- [17] E. B. Budevski, G. T. Staikov, W. J. Lorenz, Electrochemical Phase Formation and Growth: An Introduction to the Initial Stages of Metal Deposition, John Wiley & Sons, 2008.
- [18] R. Pethig, G. H. Markx, Applications of dielectrophoresis in biotechnology, *Trends Biotechnol.* 15 (1997) 426-432.
- [19] H. Siegenthaler, R. Christoph, Electrochemical Scanning Tunneling Microscope, in R.J. Behm, N. Garcia, H. Rohrer (Eds.), *Scanning Tunneling Microscopy and Related Methods*, NATO ASI Series E, Vol 184 (Kluwer, Dordrecht), 1990, pp. 315-333.
- [20] A. Alessandrini, S. Corni, and P. Facci, Unraveling single metalloprotein electron transfer by scanning probe techniques, *Phys. Chem. Chem. Phys.* 8 (2006) 4383-4397.
- [21] A. Alessandrini, M. Salerno, S. Frabboni, P. Facci, Single-metalloprotein wet biotransistor, *Appl. Phys. Lett.* 86 (2005) 133902.
- [22] R.A. Marcus, On the Theory of Oxidation-Reduction Reactions Involving Electron Transfer. I, *J. Chem. Phys.* 24 (1956) 966.
- [23] R.A. Marcus, N. Sutin, Electron transfers in chemistry and biology, *Biochim. Biophys. Acta*, 811 (1985) 265-322.
- [24] H.B. Gray, J.R. Winkler, Electron Flow through Proteins, *Chem. Phys. Lett.* 483 (2009) 1-9.
- [25] H.B. Gray, J.R. Winkler, Electron transfer in proteins, *Annu. Rev. Biochem.* 65 (1996) 537-561.
- [26] H.B. Gray, J.R. Winkler, Long-range electron transfer, *Proc. Natl. Acad. Sci. USA* 102 (2005) 3534-3539.
- [27] H. Gerischer, Über den Ablauf von Redoxreaktionen an Metallen und an Halbleitern. I. Allgemeines zum Elektronenübergang zwischen einem Festkörper und einem Redoxelektrolyten, *Z. Phys. Chem. NF*, 1960, 6, 223.
- [28] H. Gerischer, *Adv. Electrochem. Electrochem. Eng.* 139 (1961) 1.
- [29] G. Binnig, H. Rohrer, Ch. Gerber E. Weibel, Surface Studies by Scanning Tunneling Microscopy, *Phys. Rev. Lett.* 49 (1982) 57-61.
- [30] P. Lustenberger, H. Rohrer, R. Christoph H. Siegenthaler, Scanning Tunneling microscopy at potential controlled electrode surface in electrolytic environment, *J. Electroanal. Chem.* 243 (1988) 225-235.

- [31] S. Corni, A theoretical study of the electrochemical gate effect in an STM-based biomolecular transistor, *IEEE Trans. Nanotechnol.* 6 (2007) 561-570.
- [32] N. J. Tao, Probing potential-tuned resonant tunneling through redox molecules with scanning tunneling microscopy, *Phys. Rev. Lett.* 76 (1996) 4066.
- [33] J. Zhang, A. M. Kuznetsov, I. G. Medvedev, Q. Chi, T. Albrecht, P.S. Jensen, J. Ulstrup, Single-molecule electron transfer in electrochemical environments, *Chem Rev.* 108 (2008) 2737-91.
- [34] Z. Li, B. Han, G. Meszaros, I. Pobelov, T. Wandlowski, A. Blaszczyk M. Mayor, Two-dimensional assembly and local redox-activity of molecular hybrid structures in an electrochemical environment, *Faraday Discuss.* 131 (2006) 121.
- [35] T. Albrecht, A. Guckian, J. Ulstrup, J.G. Vos, Transistor-like behavior of transition metal complexes, *Nano Lett.* 5 (2005) 1451.
- [36] P. Petrangolini, A. Alessandrini, L. Berti, P. Facci, An electrochemical scanning tunneling microscopy study of 2-(6-mercaptoalkyl)hydroquinone molecules on Au(111), *J. Am. Chem. Soc.* 132 (2010) 7445.
- [37] P. Petrangolini, A. Alessandrini, M.L. Navacchia, M.L. Capobianco P. Facci, Properties of Single-Molecule-Bearing Multiple Redox Levels Studied by EC-STM/STS, *J. Phys. Chem. C* 115 (2011) 19971-19978.
- [38] J.J. Davis, B. Peters, W. Xi, J. Appel, A. Kros, T.J. Aartsma, R. Stan, G.W. Canters, Large Amplitude Conductance Gating in a Wired Redox Molecule, *J. Phys. Chem. Lett.* 1 (2010) 1541-1546.
- [39] W. Schmickler, Investigation of electrochemical electron transfer reactions with a scanning tunneling microscope: a theoretical study, *Surf. Sci.* 295 (1993) 430.
- [40] W. Schmickler, N. J. Tao, Measuring the inverted region of an electron transfer reaction with an STM. *Electrochim. Acta* 42 (1997) 2809.
- [41] J. Zhang, Q. Chi, A.M. Kuznetsov, A.G. Hansen, H. Wackerbath, H.E.M. Christensen, J.E.T. Andersen, J. Ulstrup, Electronic properties of functional biomolecules at metal/aqueous solution interfaces, *J. Phys. Chem. B* 106 (2002) 1131.
- [42] E. P. Friis, Y. I. Kharkats, A. M. Kuznetsov, J. Ulstrup, In Situ Scanning Tunneling Microscopy of a Redox Molecule as a Vibrationally Coherent Electronic Three-Level Process, *J. Phys. Chem. A* 102 (1998) 7851.
- [43] A. Migliore, A. Nitzan, Nonlinear charge transport in redox molecular junctions: a Marcus perspective, *ACS Nano*, 5, (2011) 6669-85.

- [44] B. Q. Xu, N. J. Tao, Measurement of single-molecule resistance by repeated formation of molecular junctions, *Science* 301 (2003) 1221.
- [45] I. Díez-Pérez, Z. Li, S. Guo, C. Madden, H. Huang, Y. Che, X. Yang, L. Zang, N. Tao, Ambipolar transport in an electrochemically gated single-molecule field-effect transistor, *ACS Nano*, 6 (2012) 7044-52.
- [46] W. Schmickler, C. Widrig, The investigation of redox reactions with a scanning tunneling microscope: Experimental and theoretical aspects. *J. Electroanal. Chem.* 336 (1992) 213-217.
- [47] A. M. Kuznetsov, P. Sommer-Larsen, J. Ulstrup, Resonance and environmental fluctuation effects in STM currents through large adsorbed molecules, *Surf. Sci.* 275 (1992) 52-60.
- [48] I. V. Pobelov, Z. Li, T. Wandlowski, Electrolyte gating in redox-active tunneling junctions—an electrochemical STM approach, *J. Am. Chem. Soc.* 130 (2008) 16045-16054.
- [49] I. Visoly-Fisher, K. Daie, Y. Terazono, C. Herrero, F. Fungo, L. Otero, E. Durantini, J. J. Silber, L. Sereno, D. Gust, T. A. Moore, A. L. Moore, S. M. Lindsay, Conductance of a biomolecular wire, *Proc. Natl. Acad. Sci. U.S.A.* 103 (2006) 8686-8690.
- [50] P. Petrangolini, A. Alessandrini, P. Facci, Hydroquinone-Benzoquinone Redox Couple as a Versatile Element for Molecular Electronics, *J. Phys. Chem. C* 117 (2013) 17451-17461.
- [51] Q. Chi, O. Farver, J. Ulstrup, Long-range protein electron transfer observed at the single-molecule level: In situ mapping of redox-gated tunneling resonance, *Proc. Natl. Acad. Sci. U.S.A.* 102 (2005) 16203-16208.
- [52] A. Alessandrini, M. Gerunda, G. W. Canters, M. P. Verbeet, P. Facci, Electron tunnelling through azurin is mediated by the active site Cu ion, *Chem. Phys. Lett.* 376 (2003) 625-630.
- [53] P. Facci, D. Alliata, S. Cannistraro, Potential-induced resonant tunneling through a redox metalloprotein investigated by electrochemical scanning probe microscopy, *Ultramicroscopy* 89 (2001) 291-298.
- [54] W. Haiss, T. Albrecht, H. van Zalinge, S. J. Higgins, D. Bethell, H. Höbenreich, D. J. Schiffrin, R. J. Nichols, A. M. Kuznetsov, J. Zhang, Q. Chi, J. Ulstrup, Single-Molecule Conductance of Redox Molecules in Electrochemical Scanning Tunneling Microscopy, *J. Phys. Chem. B* 111 (2007) 6703-6712.
- [55] E. Leary, S. J. Higgins, H. van Zalinge, W. Haiss, R. J. Nichols, S. Nygaard, J. O. Jeppesen, J. Ulstrup, Structure-Property Relationships in Redox-Gated Single Molecule Junctions--a Comparison of Pyrrolo-tetrathiafulvalene and Viologen Redox Groups, *J. Am. Chem. Soc.* 130 (2008) 12204-5.

- [56] I. Bâldea, Important Insight into Electron Transfer in Single-Molecule Junctions Based on Redox Metalloproteins from Transition Voltage Spectroscopy, *J. Phys. Chem. C* 117 (2013) 25798–25804.
- [57] I. Bâldea, Extending the Newns-Anderson Model to Allow transport Studies Through Molecules with Floppy Degrees of Freedom, *Europhys. Lett.* 99 (2012) 47002.
- [58] I. Bâldea, Effects of stochastic fluctuations at molecule–electrode contacts in transition voltage spectroscopy, *Chemical Physics*, 400 (2012) 65-71.
- [59] I. Bâldea, Interpretation of Stochastic Events in Single-Molecule Measurements of Conductance and Transition Voltage Spectroscopy, *J. Am. Chem. Soc.* 134 (2012) 7958–7962.
- [60] J. M. Artés, M. López-Martnez, A. Giraudet, I. Díez-Pérez, F.; Sanz, P. Gorostiza, Current-Voltage Characteristics and Transition Voltage Spectroscopy of Individual Redox Proteins, *J. Am. Chem. Soc.* 134 (2012) 20218– 20221.
- [61] E. T. Adam, Copper protein structures, *Adv. Protein Chem.* 42 (1991) 145-197.
- [62] U. Kolczak, et al. Azurin and azurin mutants, in K. Wieghardt, R. Huber, T.L. Poulos, A. Messerschmidt (Eds.), *Handbook of Metalloproteins*, (John Wiley & Sons, Chichester), 2001, pp. 1170-1194.
- [63] A. Duine, Electron Transfer from Bacterial dehydrogenases in C. Nicolini (Ed.), *From Neural Networks to Biomolecular Engineering to Bioelectronics*, (Plenum Press, New York), 1995, pp. 87-94.
- [64] Q. Chi, J. Zhang, E. P. Friis, J. E..T. Andersen, J. Ulstrup, Electrochemistry of self-assembled monolayers of the blue copper protein *Pseudomonas aeruginosa* azurin on Au(111), *Electrochem. Commun.* 1 (1999) 91-96.
- [65] H. Nar, A. Messerschmidt, M. Van De Kamp, G. W. Canters, R. Huber, Crystal structure analysis of oxidized *Pseudomonas aeruginosa* azurin at pH 5.5 and pH 9.0. A pH-induced conformational transition involves a peptide bond flip, *J. Mol. Biol.* 221 (1991) 765-772.
- [66] J.M. Artés, I. Díez-Pérez, P. Gorostiza, Transistor-like Behavior of Single Metalloprotein Junctions, *Nano Lett.* 12 (2012) 2679–2684.
- [67] J. M. Artés, M. López-Martínez, I. Díez-Pérez, F. Sanz, P. Gorostiza, *Small* 10 (2014) 2537-41.
- [68] A.G. Hansen, A. Boisen, J.U. Nielsen, H. Wackerbarth, I. Chorckendorff, J.E.T. Andersen, J. Zhang, J. Ulstrup, Adsorption and Interfacial Electron Transfer of *Saccharomyces Cerevisiae*: Yeast Cytochrome c Monolayers on Au(111) Electrodes, *Langmuir* 19 (2002) 3419.

- [69] C.A. Bortolotti, G. Battistuzzi, M. Borsari, P. Facci, A. Ranieri, M. Sola, The redox chemistry of the covalently immobilized native and low-pH forms of yeast iso-1-cytochrome c, *J. Am. Chem. Soc.* 128 (2006) 5444-51.
- [70] E.A. Della Pia, Q. Chi, D.D. Jones, J.E. Macdonald, J. Ulstrup, M. Elliott, Single-molecule mapping of long-range electron transport for a cytochrome b(562) variant, *Nano Lett.* 11 (2011) 176-82.
- [71] P. Facci, Single Metalloproteins at Work: Toward a Single-Protein Transistor, in T. Chachraborty, F. Peeters, U. Sivan (Eds.) *NanoPhysics and Bioelectronics: A New Odyssey*, Elsevier, Amsterdam, 2002, pp. 323-339.
- [72] I. Willner and E. Katz, Integration of Layered Redox Proteins and Conductive Supports for Bioelectronic Applications, *Angew. Chem. Int. Ed.* 39 (2000) 1180-1218.
- [73] M. Lösche, Protein monolayers at interfaces, *Curr. Opin. Solid State Mater. Sci.* 2 (1997) 546.
- [74] A. Ulman, Formation and structure of self-assembled monolayers, *Chem. Rev.* 96 (2001) 1533.
- [75] I. Ron, L. Sepunaru, S. Itzhakov, T. Belenkova, N. Friedman, I. Pecht, M. Sheves, D. Cahen, Proteins as electronic materials: electron transport through solid-state protein monolayer junctions, *J. Am. Chem. Soc.* 132 (2010) 4131-40.
- [76] I. Ron, I. Pecht, M. Sheves, D. Cahen, Proteins as solid-state electronic conductors, *Acc. Chem. Res.* 43 (2010) 945-53.
- [77] R. Rinaldi, A. Biasco, G. Maruccio, R. Cingolani, D. Alliata, L. Andolfi, P. Facci, F. De Rienzo, R. Di Felice, E. Molinari, Solid-State Molecular Rectifier Based on Self-Organized Metalloproteins, *Adv. Mater.* 14 (2002) 1449-1453.
- [78] R. Rinaldi, A. Biasco, G. Maruccio, R. Cingolani, D. Alliata, L. Andolfi, P. Facci, F. De Rienzo, R. Di Felice, E. Molinari, M. Verbeet, G. Canters, Electronic rectification in protein devices, *Appl. Phys. Lett.* 82 (2003) 472.
- [79] G. Maruccio, A. Biasco, P. Visconti, A. Bramanti, P.P. Pompa, F. Calabi, R. Congolani, R. Rinaldi, S. Corni, R. Di Felice, E. Molinari, M.P. Verbeet, G.W. Canters, Towards Protein Field-Effect Transistors: Report and Model of a Prototype, *Adv. Mat.* 17 (2005) 816-822.
- [80] E. D. Mentovich, B. Belgorodsky, I. Kalifa, H. Cohen, S. Richter, Large-scale fabrication of 4-nm-channel vertical protein-based ambipolar transistors, *Nano Lett.* 9 (2009) 1296-1300.
- [81] E.D Mentovich, B. Belgorodsky, S. Richter, Resolving the Mystery of the Elusive Peak: Negative Differential Resistance in Redox Proteins, *J. Phys. Chem. Lett.* 2 (2011) 1125-1128.

## Graphical abstract

